

## *r*-PROCESS IN NEUTRON STAR MERGERS

C. FREIBURGHHAUS, S. ROSSWOG, AND F.-K. THIELEMANN

Departement für Physik und Astronomie, Universität Basel, Klingelbergstrasse 82, Basel, 4058, Switzerland

Received 1999 July 20; accepted 1999 September 10; published 1999 October 6

### ABSTRACT

The production site of the neutron-rich heavy elements that are formed by rapid neutron capture (the *r*-process) is still unknown despite intensive research. Here we show detailed studies of a scenario that has been proposed earlier by Lattimer & Schramm, Symbolist & Schramm, Eichler et al., and Davies et al., namely the merger of two neutron stars. The results of hydrodynamic and full network calculations are combined in order to investigate the relevance of this scenario for *r*-process nucleosynthesis. Sufficient material is ejected to explain the amount of *r*-process nuclei in the Galaxy by decompression of neutron star material. Provided that the ejecta consist of matter with a proton-to-nucleon ratio of  $Y_e \approx 0.1$ , the calculated abundances fit the observed solar *r*-pattern excellently for nuclei that include and are heavier than the  $A \approx 130$  peak.

*Subject headings:* nuclear reactions, nucleosynthesis, abundances — stars: neutron

### 1. INTRODUCTION

It is one of the main goals of nuclear astrophysics to understand in which events the elements that constitute our physical universe are synthesized. Nuclei beyond the iron group ( $A > 90$ –100) have to be formed via successive captures of neutrons because of high Coulomb barriers for charged particle reactions. Solar abundance observations bear the imprint of only two extreme environments for neutron capture in nature: a slow (*s*-process) and a rapid (*r*-process) neutron capture process, which involve either nuclei close to ( $\tau_\beta \ll \tau_n$ ) or far from ( $\tau_\beta \gg \tau_n$ )  $\beta$ -stability.

The actual astrophysical environment for the *r*-process, however, is still unknown. The commonly suggested scenario for the *r*-process is the high-entropy (neutrino) wind of a Type II supernova (Woosley et al. 1994; Takahashi, Witt, & Janka 1994; Qian & Woosley 1996). However, recent calculations reveal two severe problems connected with this production site: the correct production of the observed *r*-process abundance pattern for nucleon numbers below 120 (Freiburghaus et al. 1997, 1999) and the heavier nuclei can only be reproduced if entropies are applied that exceed the entropy values of “state-of-the-art” supernova calculations (Takahashi et al. 1994; Meyer & Brown 1997; Hoffman, Woosley, & Qian 1997; Freiburghaus et al. 1997, 1999). There have been a number of attempts to improve this situation by changing weak interaction properties [either changing the  $\beta^-$ -decay rates (Engel et al. 1999; Martinez-Pinedo & Langanke 1999) or including neutrino capture cross sections  $\nu + (Z, A) \rightarrow (Z + 1, A) + e^-$  (Fuller & Meyer 1995; Qian, Vogel, & Wasserburg 1998)], with the aim of enhancing the “effective”  $\beta$ -decay rates that speed up the *r*-process. While this helps somewhat, it is based on the view that the *r*-process proceeds in a static way along contour lines of constant neutron separation energy that reproduce the final abundances. Then one requires about 2–3 s of process time while the supernova environment might permit less than a second. Dynamic calculations for a given entropy, however, lead to an *r*-process path initially close to the drip line (see, e.g., Freiburghaus et al. 1999) where the process timescale is not the major problem. The dominant obstacle is the required neutron-to-seed ratio that is determined by the entropy and by the rates of the reactions that fuse  $\alpha$ -particles to  $^{12}\text{C}$  (at moderate  $Y_e$ ’s of  $\approx 0.4$ ).

In an attempt to explore other astrophysical sites, we present

for the first time nucleosynthesis results of the coalescence of two neutron stars that combine detailed hydrodynamic studies, using a realistic equation of state for the neutron star material, with dynamical *r*-process calculations, which include a possible heating that is due to  $\beta$ -decays (for preliminary results, see Rosswog, Freiburghaus, & Thielemann 1999a). This scenario has been suggested earlier (Lattimer & Schramm 1974, 1976; Symbolist & Schramm 1982; Eichler et al. 1989; Davies et al. 1994) since it would provide, in a natural way, the neutron-rich environment needed for the capture reactions. In addition, it would be consistent with the observation that very old (and thus metal-poor) stars reveal a delay in the emergence of *r*-process nuclei relative to iron (Mathews, Bazan, & Cowan 1992; McWilliam 1997). This can be explained in terms of supernovae only if the *r*-process elements are produced exclusively by the lightest stars undergoing core collapse ( $7$ – $8 M_\odot$ ) because of the longer lifetimes of low-mass stars (Wheeler, Cowan, & Hillebrandt 1998). The in-spiral of a neutron star binary, however, would provide a natural explanation for this delay. Since the neutron star merger (NSM) rate is substantially lower than that of core-collapse supernovae, mergers would have to eject more material per event to explain the observations. This would cause some kind of “clumpiness” in the early distribution of *r*-process material. Such a clumpiness is actually observed (Snedden et al. 1996; Cowan et al. 1997): the relative abundances in very old stellar populations match the solar pattern very well beyond Ba, but their absolute values in comparison with Fe vary largely in different locations (up to 30 times solar).

To clarify the importance of this scenario for the *r*-process nucleosynthesis, the following questions have to be answered: (1) How often do such mergers occur? (2) How much mass is (depending on the parameters of the binary system) ejected per event? (3) How much of this material is *r*-process matter, or, respectively, how are the relative abundances distributed? The rates have recently been estimated to be  $\sim 10^{-5}$  per year and per galaxy (van den Heuvel & Lorimer 1996; Bethe & Brown 1998). We have performed Newtonian hydrodynamic calculations of the merger of two neutron stars, using the smoothed particle hydrodynamics (SPH) method (e.g., Benz 1990), where the microscopic properties of the material are described by a physical equation of state (EOS) for hot and dense nuclear matter (Lattimer & Swesty 1991). Details of the calculations

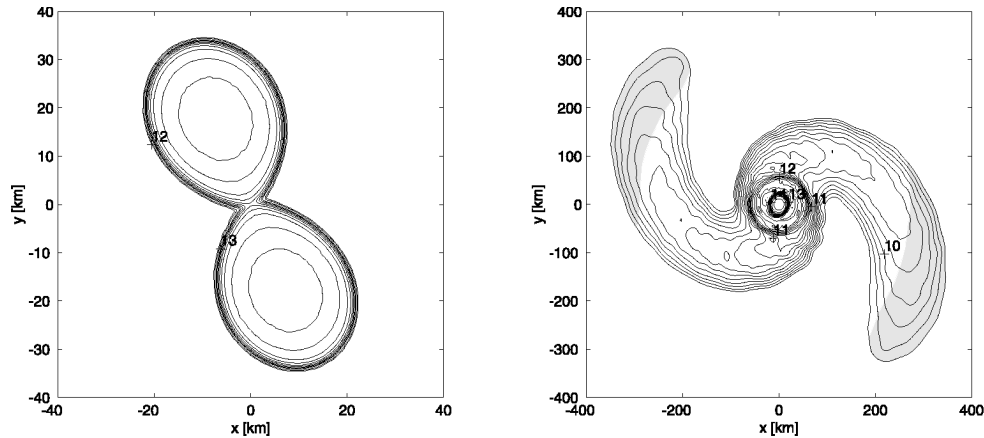


FIG. 1.—Density contours in the orbital plane of two snapshots of our calculation. The shaded region in the spiral arms marks the matter that will be ejected.

may be found elsewhere (Rosswog et al. 1999b). The main result is that between a few times  $10^{-3}$  and a few times  $10^{-2} M_{\odot}$  are ejected into space, and this is strongly dependent on the initial neutron star spins. If all the material consists of rapid neutron capture nuclei in solar proportions, this is consistent with what is needed to explain all the observed  $r$ -process material in the Galaxy exclusively by NSMs. Here we basically want to attack the remaining question (i.e., question 3) and discuss it, together with possible uncertainties.

## 2. CALCULATIONS

A few milliseconds after the neutron stars have come into contact, three different morphological regions have formed: (1) a rapidly spinning central object of  $2.5\text{--}3 M_{\odot}$ , which will probably collapse into a black hole on a millisecond timescale, surrounded by (2) a thick disk of a few times  $0.1 M_{\odot}$  and (3) a low-density region.

The intrinsic neutron star viscosity is probably too low to lead to tidal locking (like the Earth-Moon system) during the in-spiral phase of the binary, and thus spins that are negligible compared with the orbital motion are the most probable case (Bildsten & Cutler 1992; Kochanek 1992). For an irrotational binary system, we found that only around one-fourth of the material gets ejected; however, this material still could be a very interesting amount for the nucleosynthesis of heavy elements (see Fig. 26 in Rosswog et al. 1999b). Here we focus on the ejecta of the tidally locked configuration since these are best resolved and since this case is the most reliable from a numerical point of view. For these systems, all of the unbound material is located in the tips of those spiral arms (see Fig. 1).

We use a fully dynamical  $r$ -process code (Freiburghaus et al. 1999; Cowan, Cameron, & Truran 1983; Cowan, Thielemann, & Truran 1991) that accounts for possible fission cycling. As long as there are no transmutations of nuclei, the material cools by adiabatic expansion, otherwise nuclear binding energy is released and heats up the material. We used the thermodynamic history of the ejected SPH particles given in the calculations of Rosswog et al. (1999b) but added the energy input of nucleosynthesis, which leads to a temperature change. The temperature was calculated from an EOS that included electrons, positrons, photons, nucleons, nuclei, and the energy release resulting from nuclear transmutations. The entropy of the

mixture is given by

$$S(T, \rho) = S_{\gamma} + S_{e^{+}} + S_{e^{-}} + S_n + \sum_i S_i. \quad (1)$$

Apart from the nuclei, which are treated as a Maxwell-Boltzmann gas, all the other components—including neutrons—are described as a Fermi gas in order to account for the possible effects of degeneracy. The entropy source term caused by nuclear reactions is

$$dS = - \sum_{n,i} \left( \frac{m_i c^2}{k_B T} + \frac{\mu_i}{k_B T} \right) dY_i \quad (2)$$

(in units of  $k_B$  baryon $^{-1}$ ). In every time step  $t$ , the new entropy  $S(t)$  is given by adding equation (2) to the initial entropy  $S(t=0)$ . The new temperature  $T$  is given by  $S(T, \rho) = S(t)$ .

We start our nucleosynthesis calculations with conditions that are encountered when the density in the spiral arm tips has dropped below the neutron drip density ( $\rho_{\text{drip}} = 4 \times 10^{11} \text{ g cm}^{-3}$ ), which is perfectly justified since, at higher densities,  $\beta$ -decays are Pauli-blocked and no heating to  $r$ -process-like conditions may occur. We use the expansion rates found in our hydrodynamic calculations and extrapolated for times that are larger than the hydrodynamic simulation time. It is interesting to note that the density drops much faster than in the inverse free-fall expansion used in earlier calculations (Meyer 1989). This yields typical temperature histories as shown in Figure 2. The material initially cools down by means of expansion and starts to heat up again when the  $\beta$ -decays set in. We considered two extreme cases. The first case is when the temperature of the ejecta is  $T_0 \approx 6$ . This value is taken from the hydrodynamic calculation but could be incorrect since the use of the EOS by Lattimer & Swesty (1991) required (artificially) high nuclear statistical equilibrium (NSE) temperatures. As an alternative, in the second case, we considered ejected cold neutron star matter at a temperature of  $T_0 \approx 0.1$ , consisting of neutrons and protons. Figure 3 demonstrates the reheating, on extremely short timescales, to NSE temperatures that is caused by the recombination of helium and heavier nuclei for such initial conditions. In either case, the material finally cools from high temperatures (NSE) and with its corresponding seed nuclei distribution. *Thus, the encountered conditions for nucleosynthesis are independent of the initial temperatures of the ejected material.* The initial seed nuclei composition, which consists

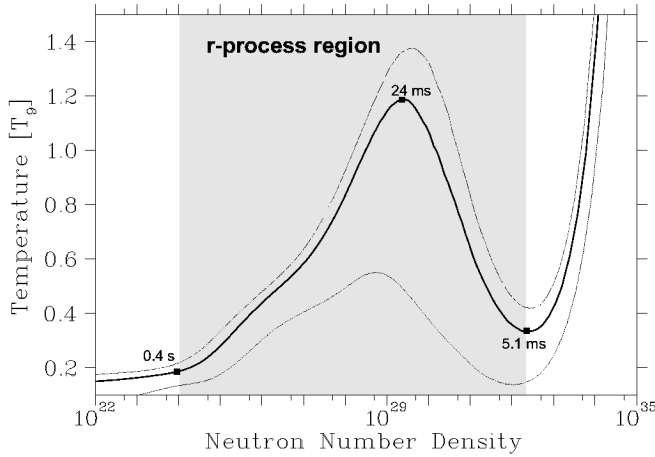


FIG. 2.—Conditions during the decompression of the neutron star material. Three cases are shown:  $Y_e = 0.12$  (thick line),  $Y_e = 0.05$  (bottom dotted line), and  $Y_e = 0.15$  (top dotted line).

of nuclei close to the neutron drip line ( $Z \approx 31\text{--}37$ ,  $A \approx 92\text{--}112$ ), is found by starting from nuclear statistical equilibrium before cooling down to the point at which Fermi blocking of  $\beta$ -decays ends and reheating sets in.

There are several uncertainties related to the  $Y_e$  of the ejected and expanding matter. In the corotating case, the ejected matter originates from the outermost layers of the neutron star. This can evolve on the order of 1% of the total neutron star mass of crust material with a  $Y_e$  up to  $\approx 0.5$  (Pethick & Ravenhall 1995; Haensel & Zdunik 1990a, 1990b). On the other hand, the outer core layers (excluding the crust) are expected to have  $Y_e < 0.05$ . Thus, the exact  $Y_e$  of the ejected matter is not fully determined unless a very fine resolution of the hydrodynamic calculation would have included the correct properties of the neutron star surface. In addition, other calculations, with varying spins of the neutron star binaries, also permit the ejection of matter from deeper layers, where a typical  $Y_e \approx 0.1$  can be found. A part of this material gets compressed and heated up when the stars come into contact. Thus, due to electron/positron capture reactions that become very effective at high temperatures, very different  $Y_e$  histories might be encountered for different initial spins. These cases demand further careful investigations of the abundance distributions.

Finally, our hydrodynamic calculation did not yet include neutrino transport, neutrino captures, or positron captures, which would have allowed us to follow the  $Y_e$  evolution more reliably. For that reason, we use  $Y_e$  in the present calculation as a free parameter in a reasonable range (0.05–0.20; see Ruffert et al. 1997). The value of  $Y_e$  has basically two effects: (1) It determines the neutron-to-seed ratio, which finally determines the maximum nucleon number  $A$  of the resulting abundance distribution, and (2) it also determines the location (neutron separation energy) of the  $r$ -process path, and thus the  $\beta$ -decay half-lives encountered; this influences the process speed and the nuclear energy release.  $Y_e$  values of 0.08–0.15 yield an almost perfect agreement with the observed  $r$ -process abundance distribution for  $A > 130$  (see Fig. 4). Higher or lower values shift the abundance peaks to incorrect positions. High  $Y_e$  values are not sufficient to achieve a full  $r$ -process. Also, very low  $Y_e$  values (like, e.g., 0.05) do not necessarily produce perfect (solar)  $r$ -process abundances, although a very strong  $r$ -process is encountered. In such a case, the neutron-to-seed ratio is so large that neutrons are not exhausted until they decay

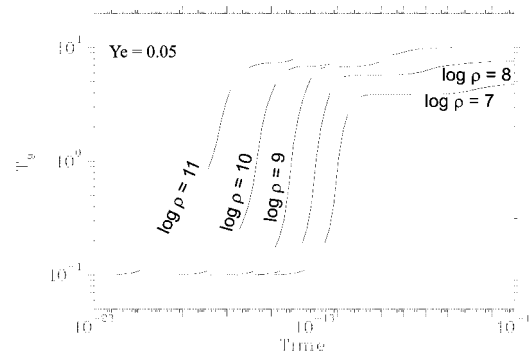


FIG. 3.—Starting at a temperature of  $T_9 \approx 0.1$ , the recombination of neutrons and protons into helium leads to a rapid heating of the material. The effect is shown for different densities. Therefore, even if the initial (high) temperatures in the hydrodynamic calculations are incorrect, low-temperature material will also immediately gain sufficiently high temperatures to come to an NSE, starting with the seed abundances deduced from the Lattimer-Swesty EOS.

with their natural half-life. However, due to the decreasing density  $\rho$  during the expansion, the neutron number density  $n_n = \rho N_A Y_n$  declines and leads to  $r$ -process paths approaching stability. This causes abundance peaks that are very close to the (solar)  $s$ -process rather than the  $r$ -process, similar to calculations in the inhomogeneous big bang (Rauscher et al. 1994). Thus, neutron star mergers create the possibility of a successful  $r$ -process site, but more detailed and self-consistent calculations are required to ensure the correct prediction of the  $Y_e$  of ejected matter.

Another interesting feature is that in the  $Y_e$  range, which reproduces the peaks nicely, there is always some amount of fission cycling that occurs, and the seed abundances and the initial mass flow below  $A = 130$  are exhausted, leading to an underproduction of the low end of the solar  $r$ -process distribution. This, however, coincides exactly with the recent finding that, in low-metallicity stars, Ag and other abundances with  $A < 130$  are underproduced, while abundances beyond Ba show a regular solar  $r$ -process pattern (Cowan et al. 1999). Evidence from meteoritic abundances also indicate that there exist two  $r$ -process sites and that one of them is responsible for all nuclei with  $A > 130$  (Wasserburg, Busso, & Gallino 1996). The NSM ejecta could be responsible for these nuclei.

### 3. SUMMARY

We have shown that NSM ejecta are a promising source of solar  $r$ -process abundances for  $A > 130$ . However, this conclusion depends on two questions that require further investigations: (1) Is the amount of ejecta folded in with the NSM merger frequency sufficient to explain the  $r$ -process matter in the Galaxy? (2) Do NSM ejecta reproduce the correct solar  $r$ -process abundance pattern? First of all, the ejecta masses from Newtonian calculations (Rosswog et al. 1999b) also have to be tested in the framework of general relativity. Second, the ejecta masses depend on the EOS employed.

Test calculations using different polytropic EOSs indicate a strong dependence of the amount of ejecta on the adiabatic exponent of the EOS, where stiffer equations result in more ejected material. If the “real” EOS should be softer than the one we used, we would then overestimate the amount of ejected material. In this case, a remedy could come from mergers of low-mass black holes with neutron stars. The most recent estimates of the corresponding rates (Bethe & Brown 1998) in-

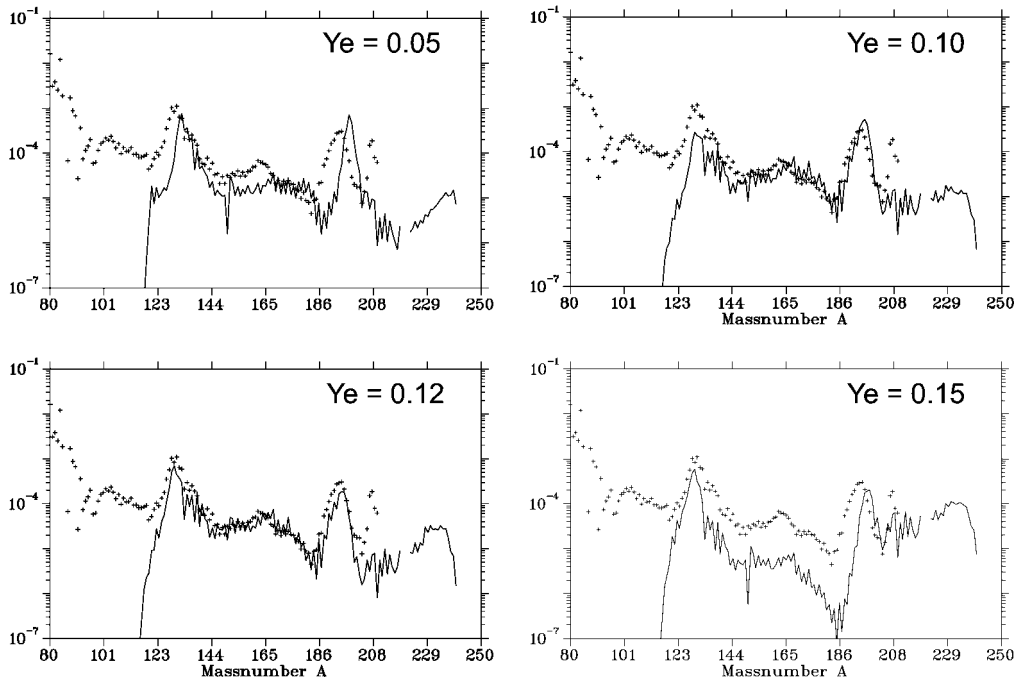


FIG. 4.—Calculated  $r$ -process distribution for different  $Y_e$ 's. In general, one obtains useful contributions for  $0.08 < Y_e < 0.15$ .

dicate that these events might be more frequent than NSMs by 1 order of magnitude. If the ejected mass for neutron star–black hole coalescences were in the same range as for NSMs and if the conditions were similar, the observations could still possibly be fitted even for a softer EOS.

While our results make the coalescence of two neutron stars an outstanding candidate for the long-sought  $r$ -process production site, the dependence of these results on  $Y_e$  underlines that further efforts have to be directed toward the full implementation of neutrinos and weak interaction cross sections as well as toward consistent hydrodynamic calculations that determine clearly the original  $Y_e$  of the ejecta. This scenario produces the correct pattern only if a  $Y_e$  range between 0.08 and

0.15 results. If the NSM scenario were responsible for the observed  $r$ -process pattern at low metallicities, one would predict a nonsolar (underabundant)  $r$ -process pattern below the  $A = 130$  peak. Therefore, future observations of these elements are highly relevant. Meteoritic and astronomical observations actually support such a behavior (Wasserburg et al. 1996; Cowan et al. 1999).

We thank W. Benz, A. Burrows, M. B. Davies, P. Höflich, H.-T. Janka, C. Pethick, and T. Piran for useful discussions. This work was supported by the Swiss NSF grant 20-53798.98 and ORNL.

#### REFERENCES

- Benz, W. 1990, in *Numerical Modeling of Stellar Pulsations*, ed. J. Buchler (Dordrecht: Kluwer), 269
- Bethe, H. A., & Brown, G. E. 1998, *ApJ*, 506, 780
- Bildsten, L., & Cutler, C. 1992, *ApJ*, 400, 175
- Cowan, J. J., Cameron, A. G. W., & Truran, J. W. 1983, *ApJ*, 265, 429
- Cowan, J. J., McWilliam, A., Sneden, C., & Burris, D. L. 1997, *ApJ*, 480, 246
- Cowan, J. J., Sneden, C., Ivans, I., Burles, S., & Beers, T. C. 1999, *BAAS*, 31, 930
- Cowan, J. J., Thielemann, F. K., & Truran, J. W. 1991, *Phys. Rep.*, 208, 267
- Davies, M. D., Benz, W., Piran, T., & Thielemann, F. K. 1994, *ApJ*, 431, 742
- Eichler, D., Livio, M., Piran, T., & Schramm, D. N. 1989, *Nature*, 340, 126
- Engel, J., Bender, M., Dobaczewski, J., Nazarewicz, W., & Surman, R. 1999, *Phys. Rev. C*, 60, 14,302
- Freiburghaus, C., Kolbe, E., Rauscher, T., Thielemann, F.-K., Kratz, K.-L., & Pfeiffer, B. 1997, *Nucl. Phys. A*, 621, 405c
- Freiburghaus, C., Rembges, J.-F., Rauscher, T., Kolbe, E., Thielemann, F.-K., Kratz, K.-L., Pfeiffer, B., & Cowan, J. J. 1999, *ApJ*, 516, 381
- Fuller, G., & Meyer, B. S. 1995, *ApJ*, 453, 792
- Haensel, P., & Zdunik, J. L. 1990a, *A&A*, 229, 117
- . 1990b, *A&A*, 227, 431
- Hoffman, R. D., Woosley, S. E., & Qian, Y.-Z. 1997, *ApJ*, 482, 951
- Kochanek, C. S. 1992, *ApJ*, 398, 234
- Lattimer, J. M., & Schramm, D. N. 1974, *ApJ*, 192, L145
- . 1976, *ApJ*, 210, 549
- Lattimer, J. M., & Swesty, D. 1991, *Nucl. Phys. A*, 535, 331
- Martinez-Pinedo, G., & Langanke, K. 1999, *Phys. Rev. Lett.*, submitted
- Mathews, G. J., Bazan, G., & Cowan, J. J. 1992, *ApJ*, 391, 719
- McWilliam, A. 1997, *ARA&A*, 35, 503
- Meyer, B. S. 1989, *ApJ*, 343, 254
- Meyer, B. S., & Brown, J. S. 1997, *ApJS*, 112, 199
- Pethick, C. J., & Ravenhall, D. G. 1995, *Annu. Rev. Nucl. Part. Sci.*, 45, 429
- Qian, Y.-Z., Vogel, P., & Wasserburg, G. J. 1998, *ApJ*, 506, 873
- Qian, Y.-Z., & Woosley, S. E. 1996, *ApJ*, 471, 331
- Rauscher, T., Applegate, J. H., Cowan, J. J., Thielemann, F. K., & Wiescher, M. 1994, *ApJ*, 429, 499
- Rosswog, S., Freiburghaus, C., & Thielemann, F.-K. 1999a, in *Nuclei in the Cosmos V*, ed. N. Prantzos & S. Harissopulos (Paris: Editions Frontières), 140
- Rosswog, S., Liebendörfer, M., Thielemann, F.-K., Davies, M., Benz, W., & Piran, T. 1999b, *A&A*, 341, 499
- Ruffert, M., Janka, H.-T., Takahashi, K., & Schäfer, G. 1997, *A&A*, 319, 122
- Sneden, C., McWilliam, A., Preston, G. W., Cowan, J. J., Burris, D. I., & Armosky, B. J. 1996, *ApJ*, 467, 819
- Symbalisty, E. M. D., & Schramm, D. N. 1982, *Astrophys. Lett.*, 22, 143
- Takahashi, K., Witt, J., & Janka, H.-T. 1994, *A&A*, 286, 857
- van den Heuvel, E., & Lorimer, D. 1996, *MNRAS*, 283, L37
- Wasserburg, G., Busso, M., & Gallino, R. 1996, *ApJ*, 466, L109
- Wheeler, J. C., Cowan, J. J., & Hillebrandt, W. 1998, *ApJ*, 493, L101
- Woosley, S. E., Wilson, J. R., Mathews, G. J., Hoffman, R. D., & Meyer, B. S. 1994, *ApJ*, 433, 229